INTERNATIONAL ATOMIC ENERGY AGENCY
UNITED NATIONS EDUCATIONAL, SCIENTIFIC AND CULTURAL ORGANIZATION

INTERNATIONAL CENTRE FOR THEORETICAL PHYSICS
34100 TRIESTE (ITALY) - P.O.B. 586 - MIRAMARE - STRADA COSTIERA 11 - TELEPHONE: 2240-1
CABLE: CENTRATOM - TELEX 460392 - I

SMR/390 - 16

WORKING PARTY ON "FRACTURE PHYSICS"
(29 May - 16 June 1989)

# BRITTLE DUCTILE TRANSITION IN SILICON

P.B. HIRSCH
University of Oxford
Dp.Metallurgy-Sc.Materials
Parks Road
Oxford OX1 3PH
United Kingdom

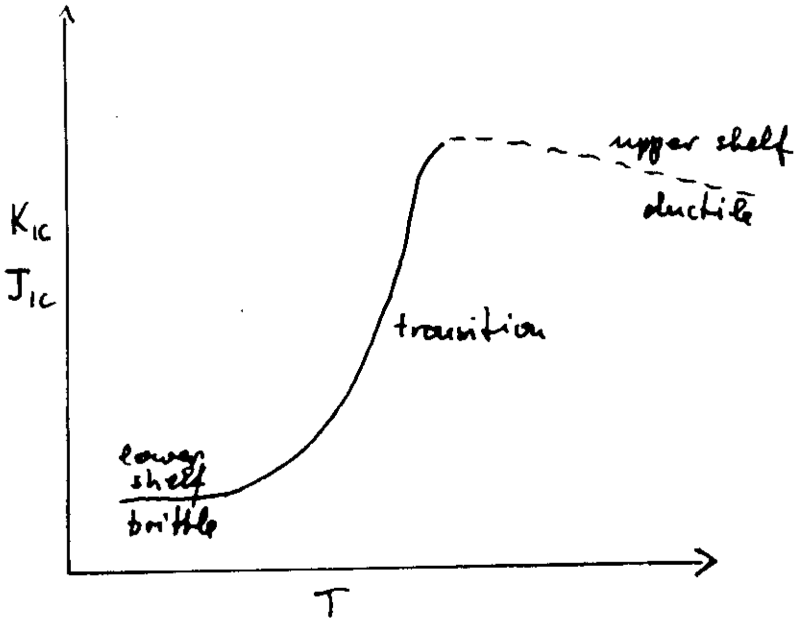


Transition curve for steels -- schematic

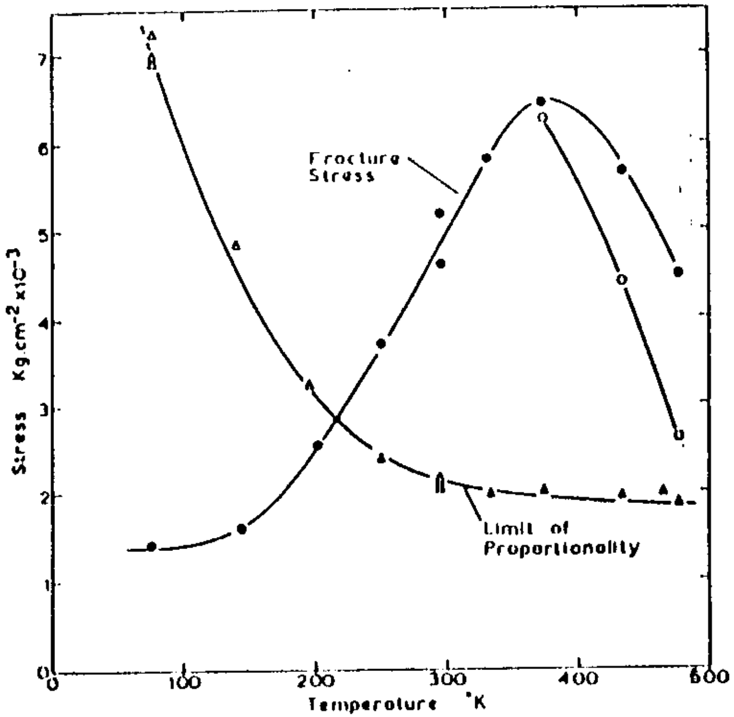


Effect of temperature on the fracture stress of pre-cracked crystals containing a constant crack length ~0·008 cm and on the limit of proportionality of uncracked and cracked crystals. ● maximum load applied; ○ load at fracture; △ limit of proportionality of uncracked crystals; ▲ limit of proportionality of precracked crystals.

T3

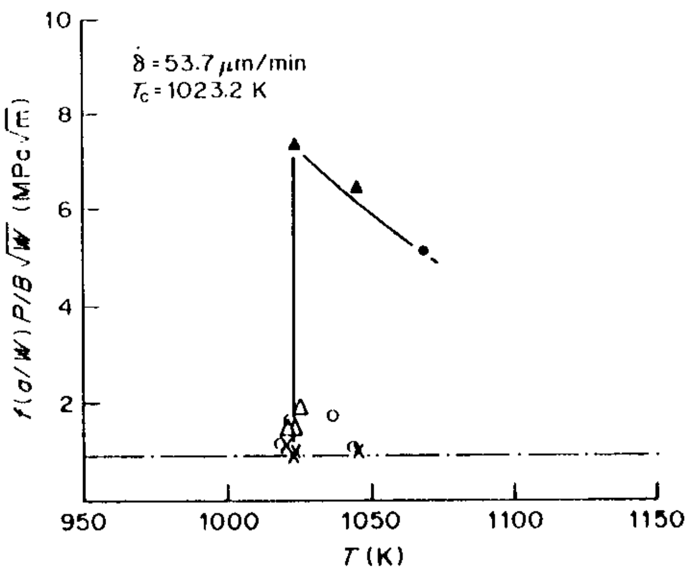


T4

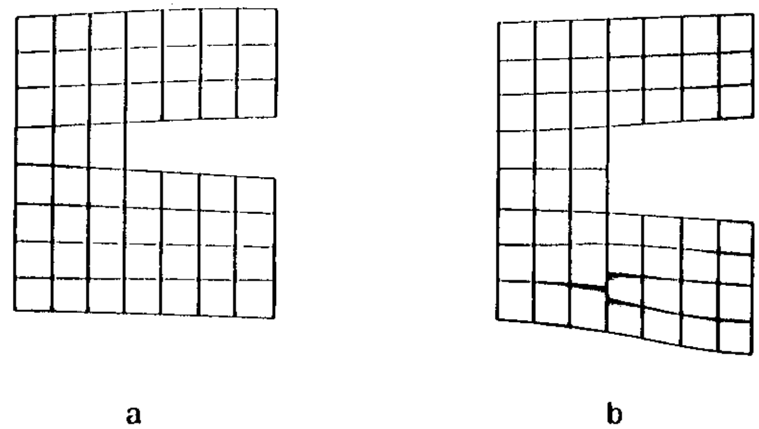


Crack-tip breakdown in shear by dislocation emission.

T5

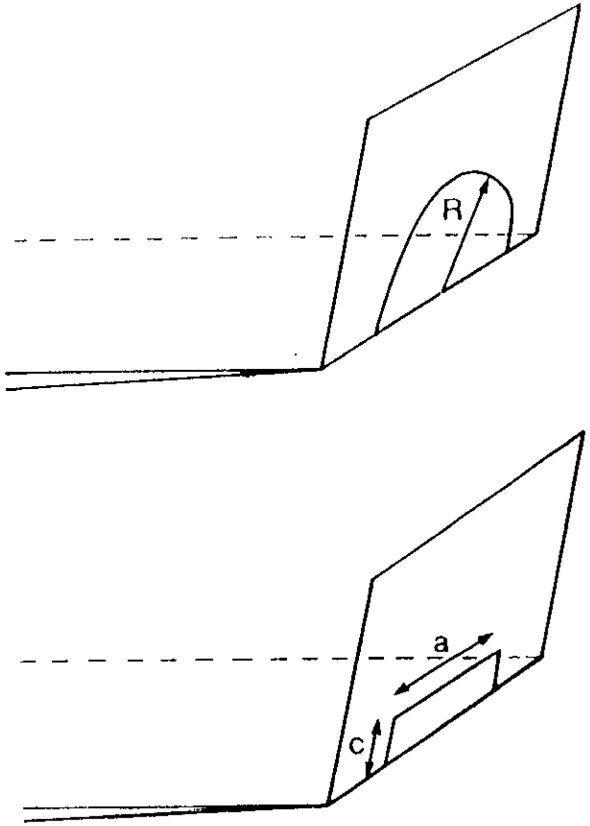


Mode-I emission in 3D. Dislocations must be nucleated from a mechanically stable rack. In (a) the shape of the critical nucleus is assumed to be a half-circle, and in (b) a rectangle.

T6

# DISLOCATION DYNAMICS AND CRACK TIP PLASTICITY AT THE BRITTLE-DUCTILE TRANSITION (BDT)

P.B. Hirsch, S.G. Roberts, J. Samuels and P.D. Warren

Department of Metallurgy and Science of Materials
University of Oxford

At the BDT plastic relaxation processes blunt and shield the cracks.
What is the controlling mechanism?
Nucleation of loops at crack tip (Rice-Thomson mechanism)?
Operation of nearby dislocation sources?

## Plan of Talk

Experimental facts for Si
Problems to be addressed
Dynamic dislocation shielding model
Role of existing dislocations
Tests of predictions of model
Conclusions.

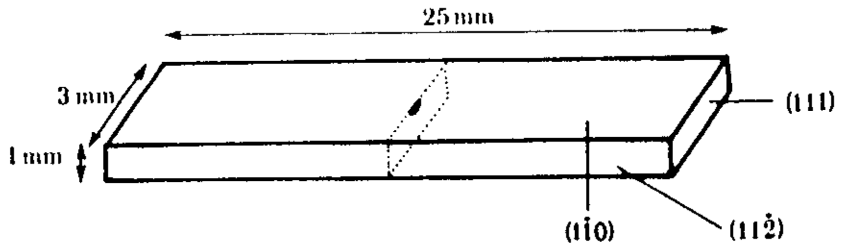


Crystallography of test specimens. A precrack is introduced on the (111) plane by Knoop indentation on the (1$\bar{1}$0) (tensile) surface (see text).



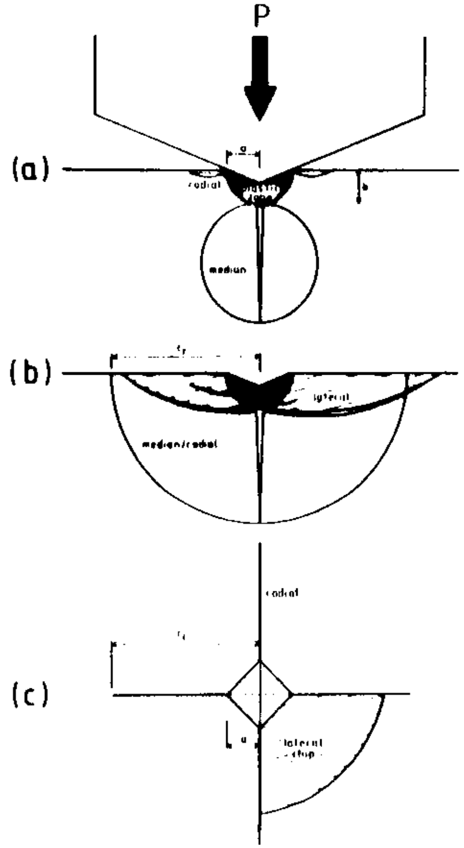


Schematic diagrams of crack geometries formed by Vickers indentations. (a) On loading the indenter above a critical load $P^*$, penny-shaped median cracks, orthogonal to the specimen surface, are nucleated at the plastic zone boundary and propagate downwards. Surface radial cracks may also form in some materials. (b) On removing the load, median cracks extend upwards and outwards and radial cracks outwards and downwards, the two crack types merging to form a composite median/radial system. In addition, lateral cracks, approximately parallel to the surface, may nucleate at the plastic zone boundary and propagate away from the indentation, forming chips of removed material where they intersect radial cracks and the specimen surface. (c) Plan view of a Vickers indentation after removal of the load, showing four radial cracks and one lateral chip. The dimensions $a$ (the indentation half-diagonal), $b$ (the plastic zone radius) and $c_r$ (the radial crack radius) are also defined in the figure.

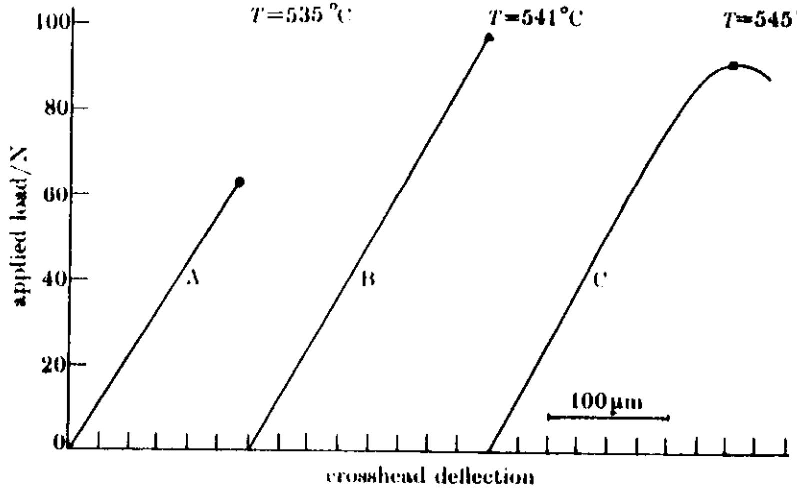


Load displacement curves for specimens tested just below (A), at (B) and just above (C) the brittle–ductile transition. Note that the 'transition' specimen fractures at a high stress, but still apparently within the elastic régime.



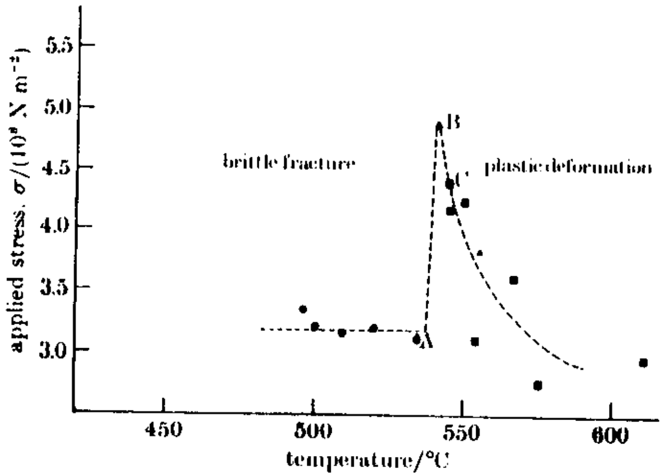


Failure stress against temperature for intrinsic silicon specimens tested at the minimum strain rate. The points marked A, B, and C correspond to the tests shown in figure 5. Note the sharpness of the brittle–ductile transition. Symbols: ●, brittle; ▲, transition; ■, ductile.

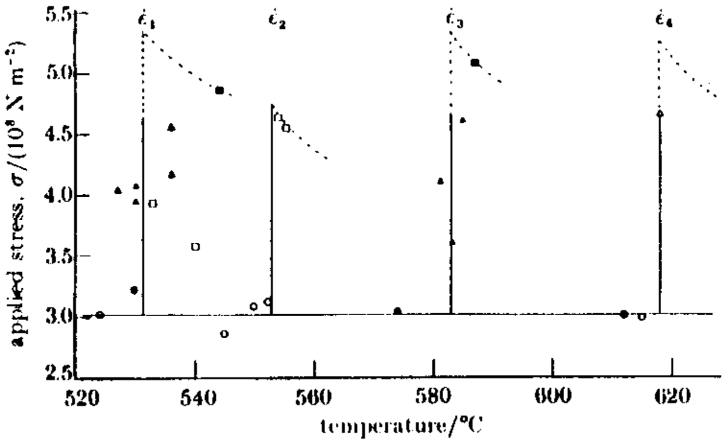


Variation of the transition temperature with strain rate for n-type ($2 \times 10^{16}$ P $cm^{-3}$) silicon: $\dot{\epsilon}_1 = 1.3 \times 10^{-6}\ s^{-1}$, $\dot{\epsilon}_2 = 2.6 \times 10^{-6}\ s^{-1}$, $\dot{\epsilon}_3 = 5.2 \times 10^{-6}\ s^{-1}$, $\dot{\epsilon}_4 = 1.3 \times 10^{-5}\ s^{-1}$. Points marked with circles, triangles and squares correspond respectively to 'brittle', 'transition' and 'ductile' tests. Two sets of experiments were performed at $\dot{\epsilon}_1$, to check consistency of results.

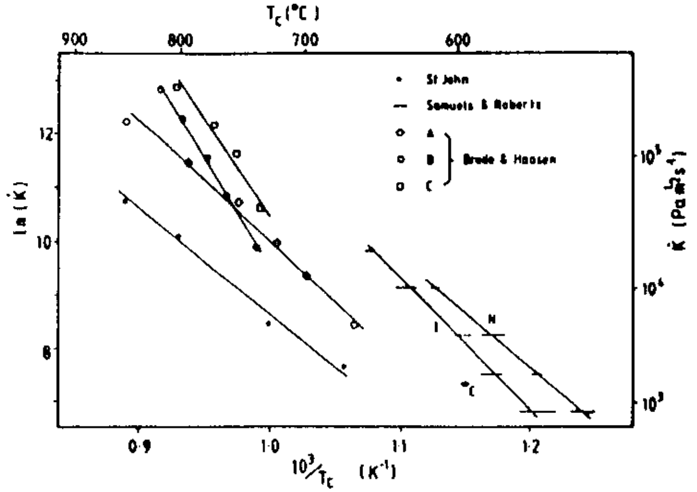


Comparison of data from the experiments of Samuels and Roberts (1989), Brede and Haasen (1988) and St. John (1975). (for doping levels see refs.)

Table 1. Activation energies

| Experiment | Activation energy Intrinsic Si ($2x10^{13}$ $Pcm^{-3}$) | n-type Si ($2x10^{18}$ $Pcm^{-3}$) |
| --- | --- | --- |
| BDT (this work) | 2.1±0.1eV | 1.6±0.1eV |
| BDT (St.John, 1975) | 1.9eV | - |
| Disln. velocity (George & Champier, 1979) | 2.2eV | 1.7eV |
| Disln. velocity (Imai & Sumino, 1983)* | 2.3eV | 1.7eV |

(* doping levels used were $2x10^{12}$ $Bcm^{-3}$ and $6.2x10^{18}$ $Pcm^{-3}$)



## Dislocation velocity and strain-rate dependence of $T_c$

The dislocation velocity v is given by

$$v = A\tau^m \exp(-U/kT) \equiv \tau^m v_o$$

where $\tau$ is the resolved stress, U the activation energy for dislocation motion, T the temperature, k the Boltzmann constant, A a constant and m a parameter which varies slowly with temperature ($m\sim1$), $v_o$ the temperature dependent term of the dislocation velocity. U depends on doping.

At the transition temperature, $T_c$, it is found that

$$\exp-(U_{BDT}/kT_c) \propto C\dot{K}$$

where $\dot{K}$ is the rate of change of the stress intensity factor in a constant strain-rate test, C is a constant, and $U_{BDT}$ is the activation energy. It is found that

$$U_{BDT} \equiv U$$

and therefore, at $T_c$

$$(\dot{K}/v_o)_{T_c} = \text{constant}.$$

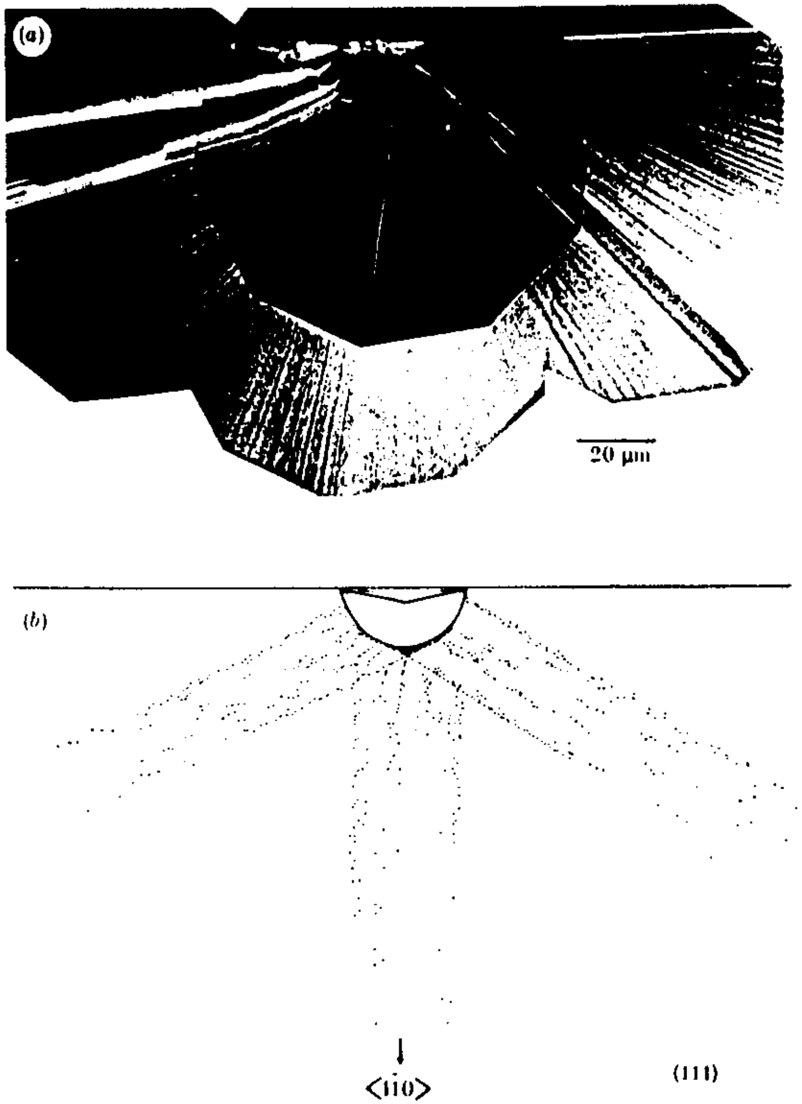


(*a*) Etched fracture face of a 'transition' specimen. (*b*) Tracing of (*a*), showing dislocation positions more clearly. Long rays of dislocations emanate from the crack front, mostly from the positions where the tangent to the crack front lies in a slip plane.



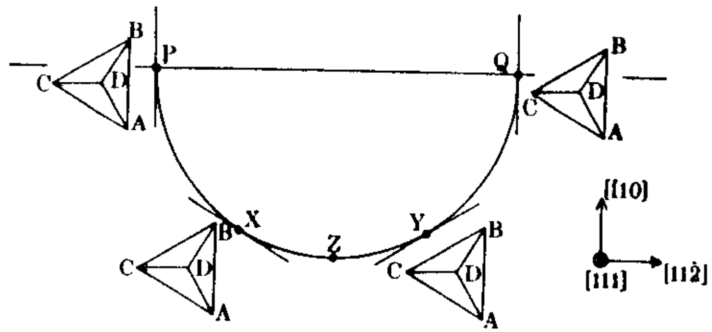


Crystallography of the precursor crack and slip planes used in the experiments. Points 'P', 'X', 'Y' and 'Q' are where a slip plane is tangential to the local crack front; 'Z' is the deepest point of the crack.

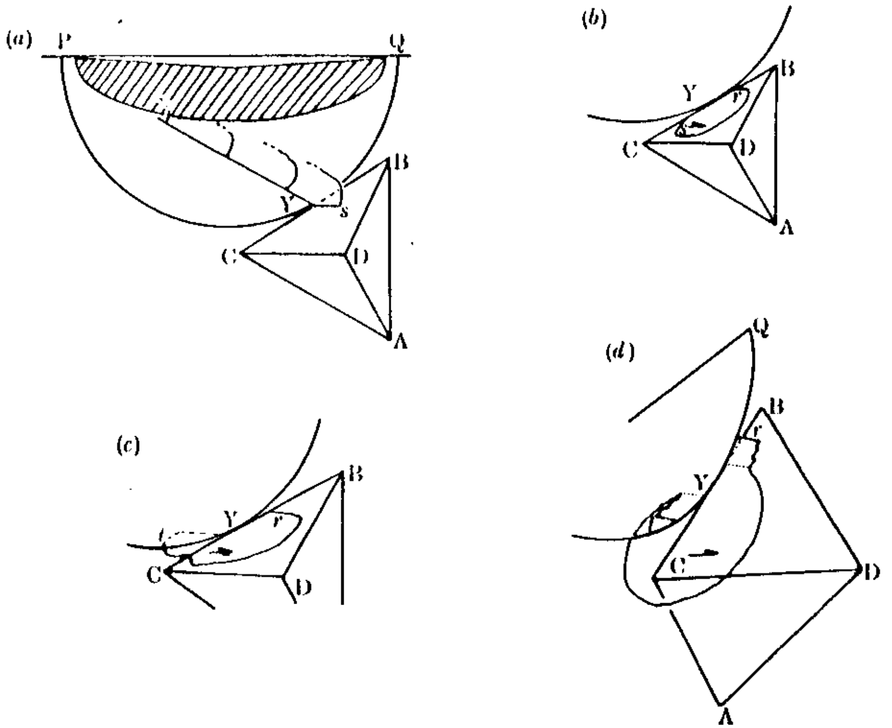


FIGURE 5. Generation and growth of a dislocation loop on the BCD plane (see text for discussion). (*a*) A segment of dislocation moves from the indentation's plastic zone to the crack front, cross slipping onto BCD. (*b*) The loop expands onto BCD. (*c*) The loop crosses the weak 'negative' stress region to expand 'behind' the crack tip. (*d*) Screw segments '*l*' and '*r*' cross slip on planes ACD and BCD to follow the crack profile.

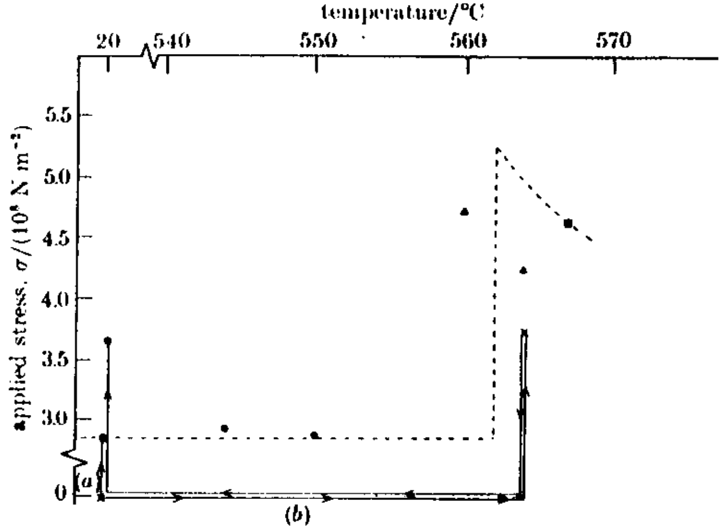


Warm prestressing in silicon, with 13 μm deep precracks. Loading at room temperature (path (*a*)) leads to fracture at the normal low-temperature fracture stress. Prestressing above $T_c$, followed by unloading and cooling to room temperature (path (*b*)) increases the room-temperature fracture stress. Symbols: ●, brittle; ▲, transition; ■, ductile. Intrinsic, $\dot{\epsilon} = 1.3 \times 10^{-6}\ s^{-1}$.

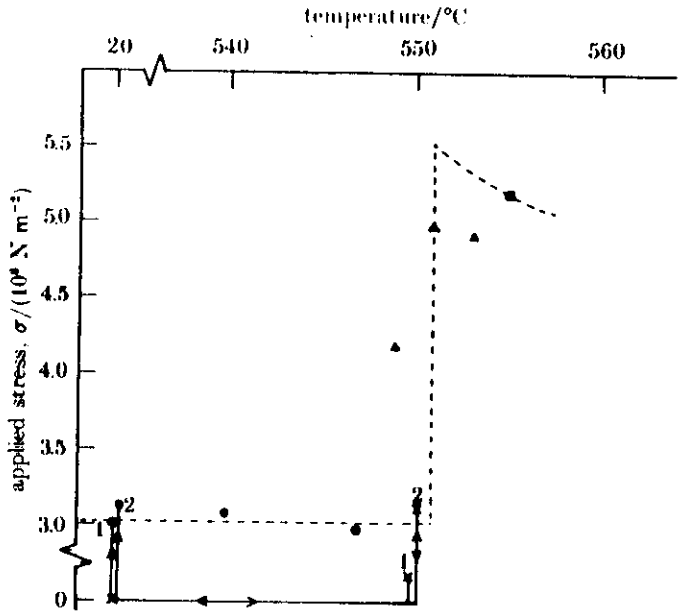


Determination of the conditions for dislocation emission in dynamic tests near $T_c$. A specimen prestressed to 0.9 $K_{1c}$ (1) fractures at the normal room-temperature fracture stress, indicating that no dislocations have been emitted from the crack tip. A specimen prestressed to 1.1 $K_{1c}$ (2) shows a small warm-prestressing effect, indicating that in this case dislocations have been emitted. Symbols: ●, brittle; ▲, transition; ■, ductile. P-type, $\dot{\epsilon} = 1.3 \times 10^{-6}$ s$^{-1}$.



## Problems to be addressed

1. At BDT $\dot{K} \propto v_o$.

2. BDT for Si is very sharp - why?

   No dislocation activity a few degrees below $T_c$.

   Little dislocation activity at $T_c$ for K $\leq$ 0.9 $K_{1c}$.

3. At $T_c$ brittle fracture can occur at K > $K_{1c}$.

   How can cleavage occur after plastic flow?

   What is the criterion for brittle fracture at BDT?

4. What is the role of existing dislocations in the crystal?

T21 CH

T22 DH

## DYNAMIC DISLOCATION SHIELDING MODEL FOR BDT

Dislocation loops emitted from crack tip sources shield the crack.

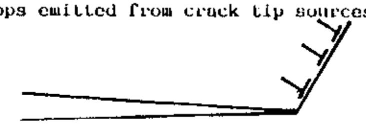

### Conditions for brittle fracture

Total force on crack tip.

1. $f_c = \frac{K_{eIII}^2}{2\mu} + \frac{(1-\nu)}{2\mu}(K_{eI}^2 + K_{eII}^2) \geq \frac{(1-\nu)}{2\mu} K_{Ic}^2$

   $K_{eI}$, $K_{eII}$, $K_{eIII}$ - local stress intensity factors in modes I, II, III.

   $K_{Ic}$ - critical stress intensity factor for low temperature brittle fracture in mode I.

   $\mu$ - shear modulus.

   $\nu$ - Poisson's ratio

2. Instability criterion $\frac{df_c}{da} > 0$.

### In mode I:

$K_{eI} = K_I - K_{DI}$

$K_{eII}^2 = K_{DII}^2$

$K_{eIII}^2 = K_{DIII}^2$

$K_I$ - applied stress intensity factor

$K_{DI}$, $K_{DII}$, $K_{DIII}$ - dislocation shielding terms

### Simplified Models

Mode III:- $K_e = K_I - K_{DIII} \geq K_{Ic}$

Mode I:- $K_{eI} = K_I - K_{DI} \geq K_{Ic}$

Instability criterion satisfied for Mode I.

### Criterion for BDT

The BDT occurs at the lowest temperature (for a given strain rate) for which $K_e < K_{Ic}$ up to a value of $K_I$ at which macroscopic yield takes place.

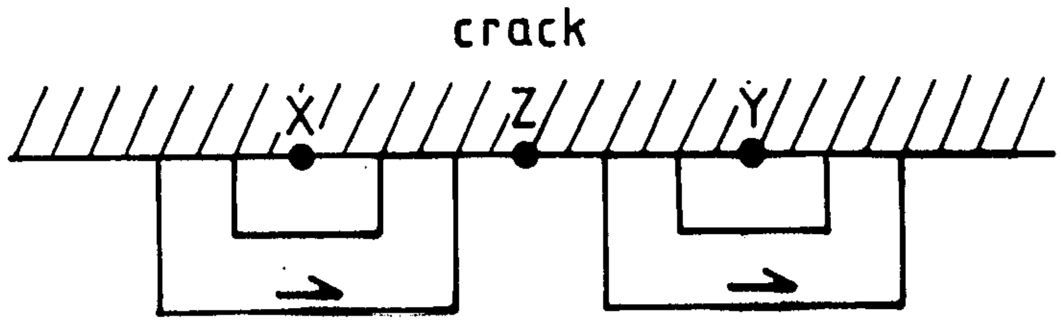


Simplified model of the crack front and dislocation loops used for the computer simulation. Loops expand from points 'Y' and 'X', eventually to cover point 'Z'.

T23 EH

## Assumptions in Dynamic Dislocation Shielding Model

Replace Mode I deformation by Mode III deformation.

Dislocations emitted from 2 sources.

Replace curved crack profile by straight crack profile.

Velocity of edge dislocation same as for screws.

Dislocation interaction stresses are those between parallel screws.

T24 FH

## Dynamic Dislocation Shielding Model

On these assumptions, stress on any dislocation at $x_i$ is

$$\tau_{x_i} = \frac{K}{(2\pi x_i)^{1/2}} - \frac{\alpha\mu b}{x_i} + \frac{\mu b}{2\pi}\sum_{j\neq i}\left(\frac{x_j}{x_i}\right)^{1/2}\frac{1}{(x_i - x_j)}$$

where $x_i$ is position of ith dislocation, $\alpha$ the line tension/image stress parameter, $\mu$ the shear modulus, b the Burgers vector. The first term is the crack tip stress, the second the line tension/image stress, the third the dislocation/dislocation interaction.

Dislocation velocity is

$$\frac{dx_i}{dt} = A\tau^m \exp{-U/kT} = \tau^m v_o$$

With

$$\frac{dx_i}{dt} = \dot{K}\frac{dx_i}{dK}$$

we find

$$(\dot{K}/v_o)^{1/m}\left(\frac{dx_i}{dK}\right)^{1/m} = \frac{K}{(2\pi x_i)^{1/2}} - \frac{\alpha\mu b}{x_i} + \frac{\mu b}{2\pi}\sum_{j\neq i}\left(\frac{x_j}{x_i}\right)^{1/2}\frac{1}{(x_i - x_j)}$$

In constant strain rate test $\dot{K}$ is constant, and positions of dislocations can be uniquely determined as function of K. Shielding at source

$$K_{es} = K - \Sigma K_D = K - \sum_j \frac{\mu b}{(2\pi x_j)^{1/2}}$$

Dynamic Dislocation Shielding Model

Mode I; slip plane at 90° to crack plane

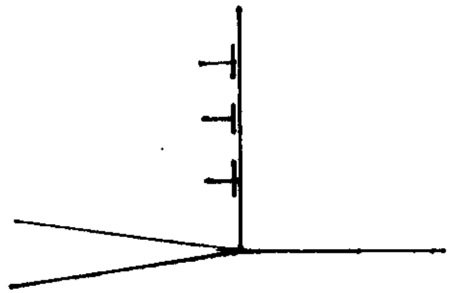

$$\tau_{x_i} = \frac{K}{2(4\pi x_i)^{1/2}} - \frac{\alpha\mu b}{4\pi(1-\nu)x_i} + \frac{\mu b}{4\pi(1-\nu)} \sum_{j\neq i} \left(\frac{x_j}{x_i}\right)^{1/2} \frac{1}{(x_i - x_j)} + \frac{\mu b}{4\pi(1-\nu)} \sum_{j\neq i} \frac{8 x_i x_j^2}{(x_i+x_j)^3 (x_i - x_j)}$$

Shielding

$$K_{es} = K - \Sigma K_D = K - \sum_j \frac{3\mu b}{2(1-\nu)(4\pi x_j)^{1/2}}$$

CONDITIONS FOR NUCLEATION OF DISLOCATION LOOP

Stress at critical distance $x_c$ from the tip must be sufficient to expand the loop

$$\frac{K}{(2\pi x_c)^{1/2}} \geq \frac{\alpha\mu b}{x_c} - \frac{\mu b}{2\pi} \sum_j \left(\frac{x_j}{x_c}\right)^{1/2} \frac{1}{(x_c - x_j)}$$

First dislocation emitted at a critical value of

$$K = K_N = \alpha\mu b(2\pi/x_c)^{1/2}$$

Calculations are performed for different $K_N$ by changing $\alpha$ or $x_c$.

SHIELDING AT VULNERABLE POINT Z ON CRACK FRONT

$$K_{oz} = K - \sum_{j>j_o} \frac{\mu b}{(2\pi x_j)^{1/2}}$$

summing over all dislocations which have moved past Z.

Note that this builds into the model a dislocation-free zone at Z, equal to XZ.

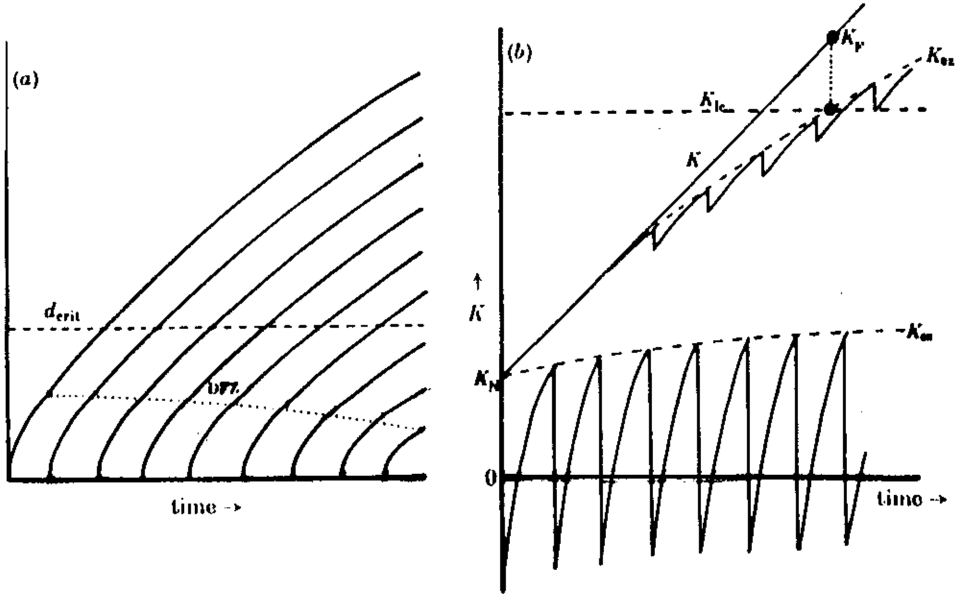


GURE 7. Schematic illustration of the main features of the computer simulation. (*a*) Positions of dislocations as a function of time; they rapidly cross the 'dislocation-free zone' to join the moving inverted pile-up. At $d_{crit}$, a dislocation can shield point 'Z'. (*b*) Variation with time of applied and effective stress intensity values. Effective $K$ at the source ($K_{es}$) rises and falls as each dislocation is emitted, but stays close to $K_N$. The effective $K$ at point 'Z' ($K_{ez}$) diverges from the applied $K$ once dislocations have passed $d_{crit}$. $K_{ez}$ eventually rises above $K_{Ic}$; at this point the applied $K$ is at $K_F$.

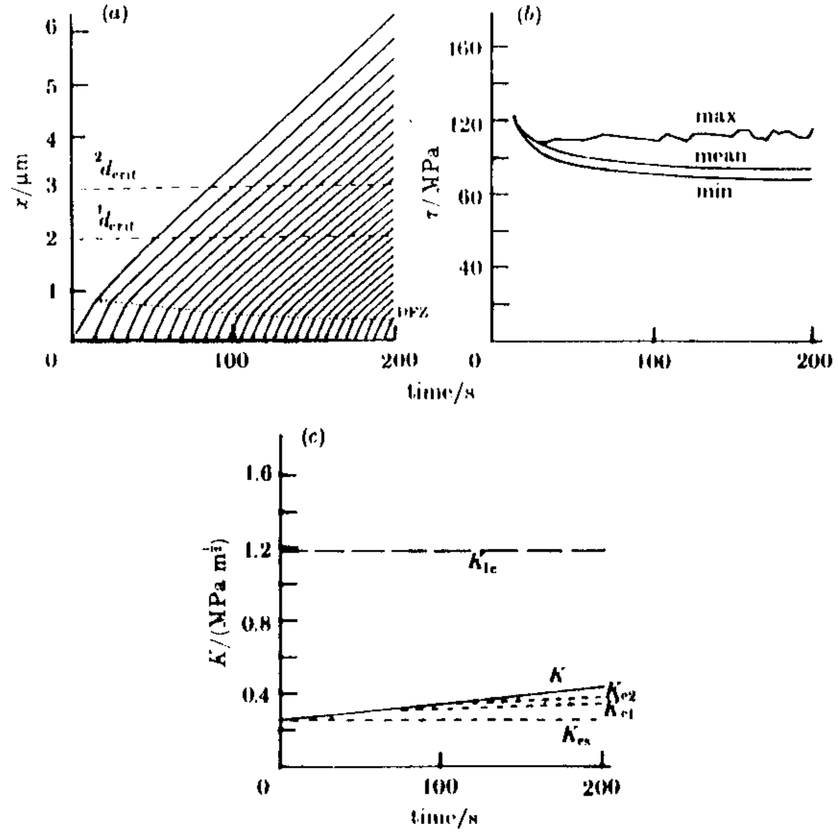


Output from the computer simulation for $K_0 = K_N = 0.21\ K_{Ic}$, 550 °C, $\dot{K} = 886\ \mathrm{Pa\ m^{1/2}\ s^{-1}}$. (*a*) Dislocation positions; note the dislocations rapidly cross the 'dislocation-free' zone (DFZ) to join the moving pile-up. (*b*) Stresses on the dislocations. The mean and minimum stresses decrease slowly with time; the maximum stress varies depending on the position of the associated dislocation in the DFZ. (*c*) Stress intensities. The applied $K$ rises linearly with time, $K_{es}$ stays close to $K_N$ (0.21 $K_{Ic}$), and $K_{ez}$ values for the two values of $d_{crit}$ shown in figure 8*a* diverge slowly from applied $K$.

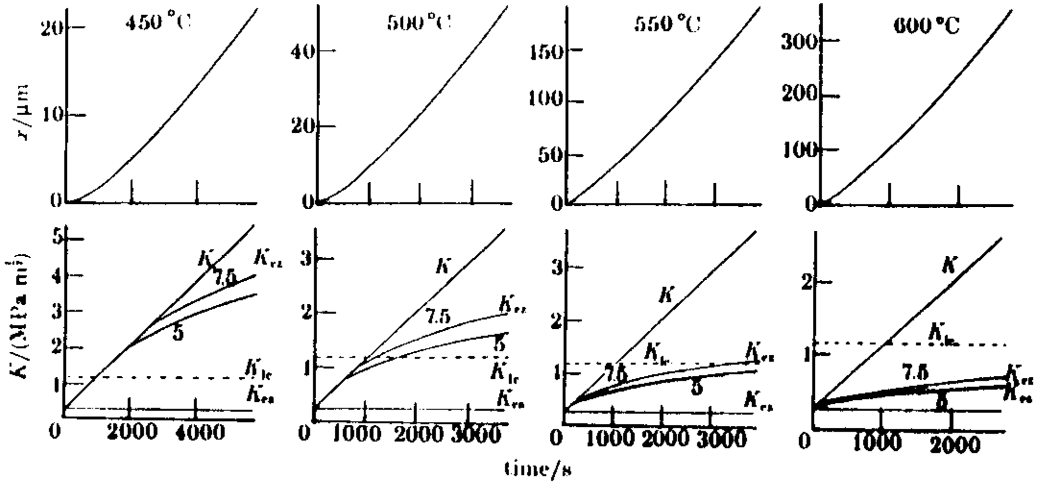


Computer simulations for $K_N = 0.2\,K_{Ic}$, for four temperatures close to the brittle–ductile transition. The upper graphs show the position of the leading dislocation, and the lower graphs applied $K$, $K_{es}$ and $K_{et}$ for two values of $d_{crit}$ (5 μm and 7.5 μm). The model predicts brittle behaviour at 450 °C, transition behaviour at 500 °C and 550 °C; the long-term behaviour at 600 °C is uncertain.

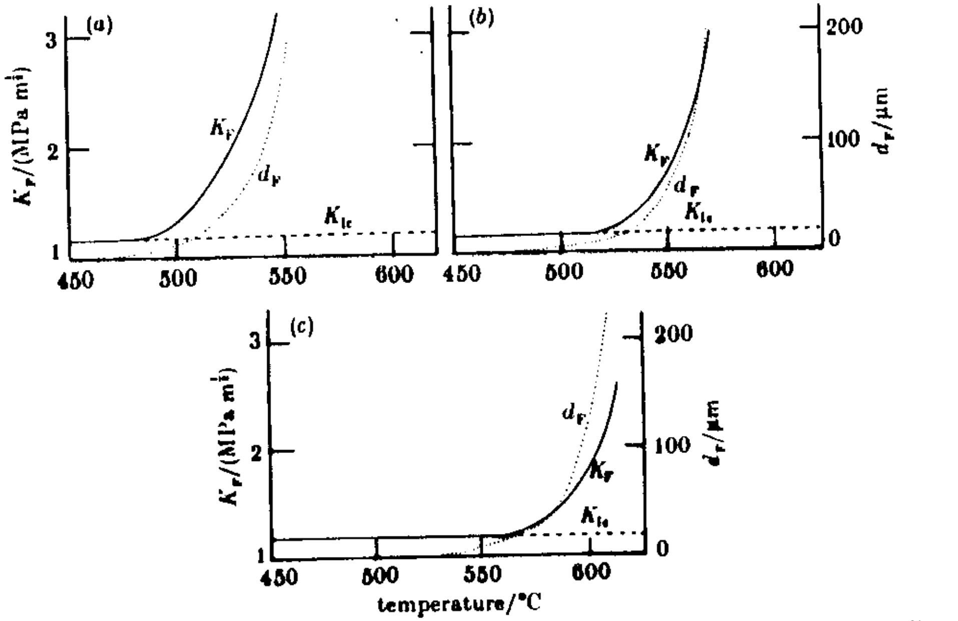


Predictions of applied $K$ (solid lines) and extent of dislocation array (dotted lines) at fracture for three different values of $K_N$. A smooth brittle–ductile transition is predicted for all values of $K_N$, the transition temperature increasing with increasing $K_N$. (a) $K_N = 0.2\,K_{Ic}$; (b) $K_N = 0.75\,K_{Ic}$; (c) $K_N = 0.95\,K_{Ic}$.

T31

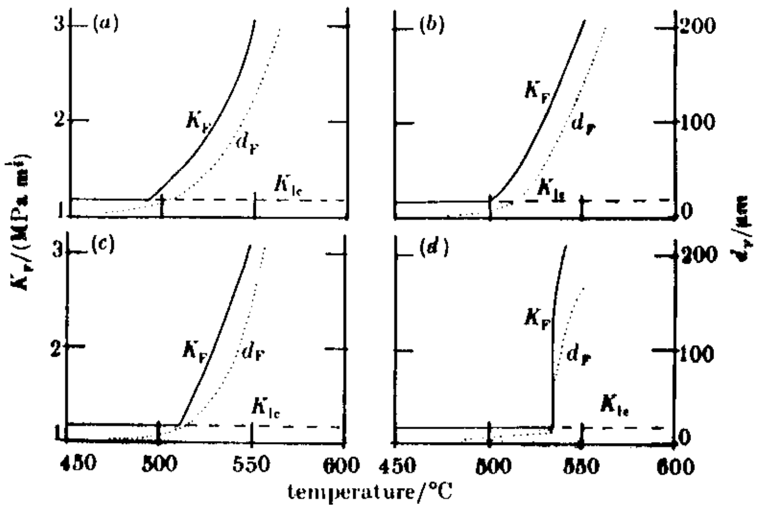


Variation of BDT with $K_0$ (*a*) $K_0 = 0.2\ K_{Ic}$; (*b*) $K_0 = 0.75\ K_{Ic}$; (*c*) $K_0 = 0.85\ K_{Ic}$; (*d*) $K_0 = 0.95\ K_{Ic}$. $\dot{K} = 0.21\ K_{Ic}$ in all cases. Predictions of applied $K$ (solid lines) and extent of dislocation array (dotted lines) at fracture for four different values of $K_0$. A smooth brittle–ductile transition is predicted for low values of $K_0$, with the transition becoming sharp as $K_0$ approaches $K_{Ic}$.

T32

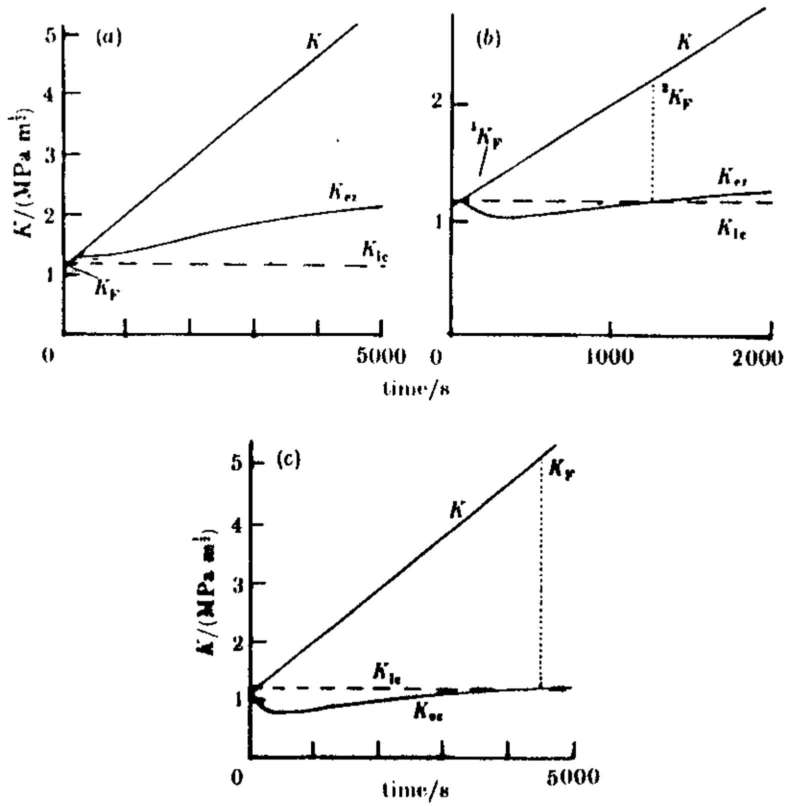


Characteristics of a sharp brittle–ductile transition. $K_{et}$ is shown as a function of time for three temperatures. (*a*) 510 °C; brittle. $K_{et}$ reaches $K_{Ic}$ before dislocations pass $d_{crit}$ (7.5 μm). (*b*) 535 °C; transition. $K_{et}$ diverges from applied $K$ exactly at $K_{Ic}$ ($K_{F1}$), drops rapidly and later rises to reach $K_{Ic}$ with applied $K = K_{F2}$. (*c*) 570 °C; ductile. $K_F$ is high; the associated stress level is above that for general yielding. Note that an increase in temperature from just below to just above 535 °C will produce a jump in $K_F$ from $^1K_F$ (= $K_{Ic}$) to $^2K_F$.

## EXPERIMENTAL AND CALCULATED VALUES OF NUMBERS OF DISLOCATIONS (N) AND DISTANCES TRAVELLED ($d_f$) AT FRACTURE

| | | N | $d_f$ ($\mu$m) |
|---|---|---|---|
| **Experiments** | | | |
| | $\dot{K}=886 Nm^{-3/2}s^{-1}$; $T_c$ ~535°C; $K_F$ =1.6PMam$^{\frac{1}{2}}$ | ~100 | ~100 |
| **Calculations** | | | |
| Mode III | $K_o$ ~0.9$K_{Ic}$; $K_N$ =0.2$K_{Ic}$; $T_o$ ~525°C; $K_F$ ~1.6PMam$^{\frac{1}{2}}$ | ~350 | ~30 |
| Mode I | $K_o$ =0.98$K_{Ic}$; $K_N$ =0.2$K_{Ic}$; $T_o$ =570°C; $K_F$ ~1.5MPam$^{\frac{1}{2}}$ | ~150 | ~40 |



## Nucleation Model - Effect of existing dislocations

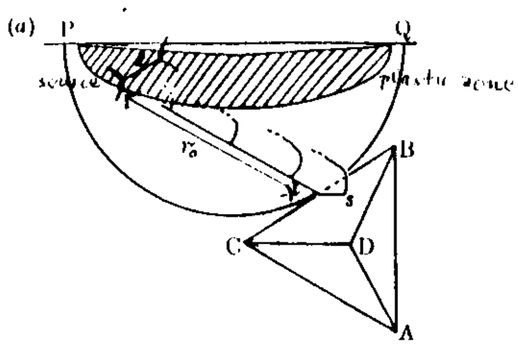


Source in plastic zone under indenter operates at a stress $\tau_d = \mu b/l$, where $\mu$ = shear modulus, b = Burgers vector, l = source length. If the source is at $r_o$ from the crack tip, it will operate at a stress intensity factor

$$K_d = ((8\pi r_o)^{\frac{1}{2}}/f)\mu b/l$$

where f is an orientation factor.

When the dislocation reaches the crack tip it forms a crack tip source, which shields the crack efficiently.

Existing dislocations can control the BDT only if $K_d < K_{1c}$.

## Model for nucleation of crack-tip source

Dislocation at $r_o$ from crack tip starts moving at $K=K_d$, and reaches crack tip at $K_o$, where

$$K_o^{m+1} - K_d^{m+1} = \frac{2(m+1)(8\pi)^{m/2} r_o^{(1+m/2)}}{(m+2)\ f^m} \left(\frac{\dot{K}}{v_o}\right)$$

where f = orientation factor. $K_d$ depends on dislocation source length $\ell$ in crystal, i.e.

$$K_d = ((8\pi r_o)^{\frac{1}{2}}/f)\mu b/\ell$$

Note

1. Provided $K_d$, $r_o$, f are constant for given structure, $K_o$ is function only of $(\dot{K}/v_o)$, so that at $T_c$, $(\dot{K}/v_o)$ = constant, as observed.
2. For experimental values $r_o = 13.3\mu m$, $\ell/b \sim 10^4$, $K_d \sim 0.46 MPam^{\frac{1}{2}}$.
3. Writing $\exp(-U/kT_c) = C\dot{K}$

   $$C = \frac{2(m+1)(8\pi)^{m/2} r_o^{(1+m/2)}}{(m+2)f^m A(K_o^{m+1}-K_d^{m+1})}$$

   C can be calculated and compared with experiment; $(K_o \sim K_{Ic})$.
4. A size effect is predicted - the larger $r_o$ the smaller $\dot{K}/v_o$, and therefore $T_c$ higher.
5. Existing dislocations can control BDT only if $K_d < K_{Ic}$,

   i.e. $r_o^{\frac{1}{2}} < (K_{Ic} f/(8\pi)^{\frac{1}{2}}\mu)(\ell/b)$

   For Si, for $\ell/b \approx 10^4$, f = 0.7, $r_o$ < 650$\mu m$



TABLE 1 CALCULATED AND EXPERIMENTAL VALUES OF ln(C)
[Units of C are $sPa^{-1}m^{-\frac{1}{2}}$]

| | intrinsic ($2\times10^{13}Pcm^{-3}$) | n-type ($2\times10^{18}Pcm^{-3}$) |
|---|---|---|
| Calculated from equation (20) | -35.8 | -30.2 |
| Experimental values from figure 10 in I | -36±1 | -31±1 |

TABLE 2 CALCULATED AND OBSERVED TRANSITION TEMPERATURE $T_c$

| | | | |
|---|---|---|---|
| $r_o$ ($\mu m$) | 13.3±0.9 | 13.3±0.9 | 37.4±1.4 |
| $\dot{K}$ ($Pam^{\frac{1}{2}}s^{-1}$) | 886 | 1487 | 1487 |
| $T_c$ (°C)(from eqn. 19) | 561±3 | 577 | 628±2 |
| $T_c$ (°C)(experimental) | 560±5 | 576±5* | 598±2 |

*(Interpolated)

T37

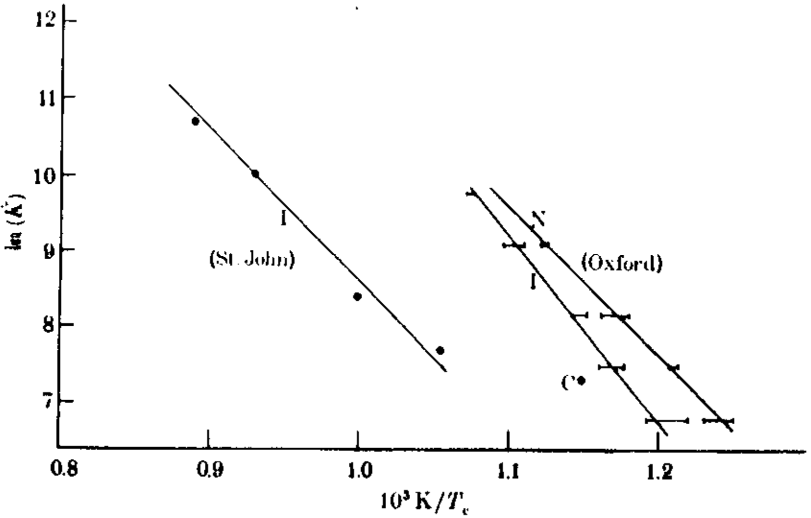


Arrhenius plot comparing the results of figure 10 to those of St. John (1975); all data are here plotted on a common scale of ln ($\dot{K}$) against $1/T_c$. Although the two sets of results for intrinsic silicon give similar activation energies (slope), St. John's results consistently give higher values of $T_c$ (by *ca.* 100 °C) in the overlapping strain rate range. The point 'C' is for intrinsic silicon with a larger precursor crack size (37 μm); this point does not lie on the line for specimens with the standard crack size (13 μm) (see text). Abbreviations: I, intrinsic; N, n-type.

T38

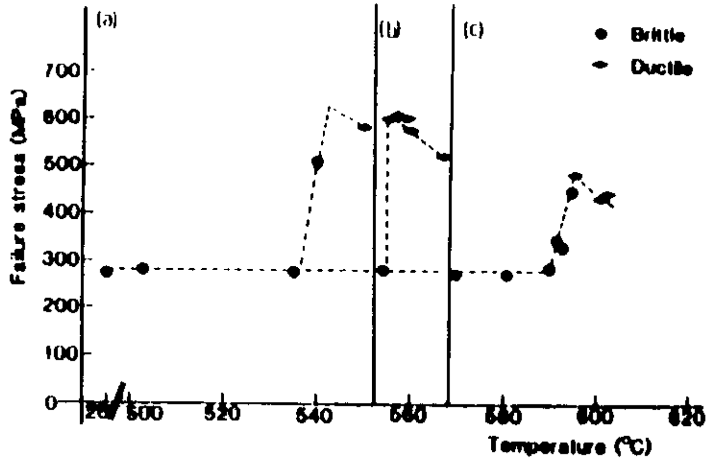


Failure stress versus temperature for:
(a) 'Control' specimens. $T_c$=545°C;
(b) 'Abraded' specimens $T_c$=555°C.
(c) 'Polished' specimens. $T_c$=595°C;

T 39

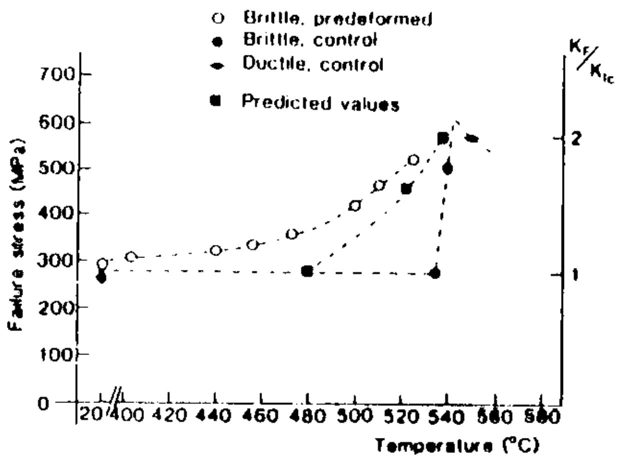


Failure stress versus temperature for pre-deformed specimens compared with 'normal' specimens, and a computer simulation.

T40 C4

## ROLE OF EXISTING DISLOCATIONS

1. $T_c$ is predicted to decrease with increasing dislocation density, increase with decreasing dislocation density.

2. Where crack tip sources are already present, nucleation is not necessary, and transition should be gradual (BCC metals).

3. Crack tip sources provide more efficient shielding than sources in the bulk. Existing bulk sources can control the BDT by emission of dislocations which form crack tip sources. Existing dislocations can control the BDT only if $K_d < K_{1c}$. For Si, e.g. for $\ell/b \approx 10^4$, $f = 0.7$, $r_o < 650\mu m$. If $K_d > K_{Ic}$, nucleation of loops at crack tips by the Rice-Thomson mechanism may control. Observed in thin foils by TEM (Ohr, Chiao and Clarke).

## Nucleation Model - Lüders type band propagation

Suppose that dislocations are emitted at special sites along the crack, e.g. at the surface. Loops emitted from these sites help to activate potential sources at other, more difficult sites, along the crack.

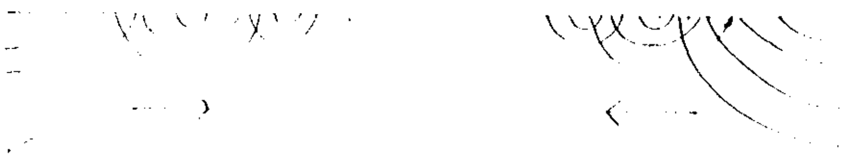

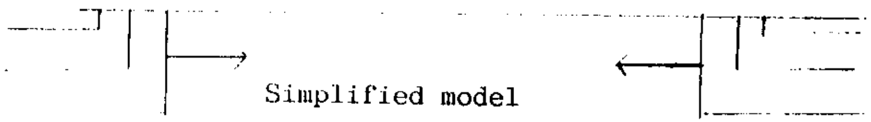

Simplified model

## Criterion for BDT:

Loops must traverse ${}_i d_{crit}$ before $K=K_{Ic}$. This criterion determines $T_c$. The distance $(2\,{}_i d_{crit})$ between the original sources may be ~ crystal thickness, if slip starts at the surface; after traversing to the centre, the distance between active sources $({}_f d_{crit})$ may be very small (say ~1μm). The sharpness of the transition is controlled by ${}_f d_{crit}$.

| $\dot{K}/\dot{K}_0$ | 0.3 | 1.8 | 2.8 | 10.0 | |
|---|---|---|---|---|---|
| $T_c$ (exp) | 946 | [illegible] | [illegible] | 1075 | (K) |
| $\tau$ (exp) | 10 | 14.6 | 16.3 | 13.1 | (MPa) |
| $T_c$ (model) | 945 | [illegible] | 1045 | 1090 | (K) |
| $\tau$ (model) | 10 - 11 | 10 - 12 | 10-12 | 9 - 14 | (MPa) |
| $\dot{d}$ (model) | 0.8 | 2.8 | 6 | 30 | $(10^{-7}\,m\,s^{-1})$ |
| $\dot{d}\,/\,\dot{K}/\dot{K}_0$ | 2.7 | 2.8 | 3.0 | 3.0 | $(10^{-7}\,m\,s^{-1})$ |

$(\dot{K}_0 = 310\ MPa\sqrt{m}\,s^{-1})$

for the model, $K_N = K_0 = 0.3K_{Ic}$, $K_{Ic} = 0.93\ MPa\sqrt{m}$, $d_{crit} = 550\mu m$

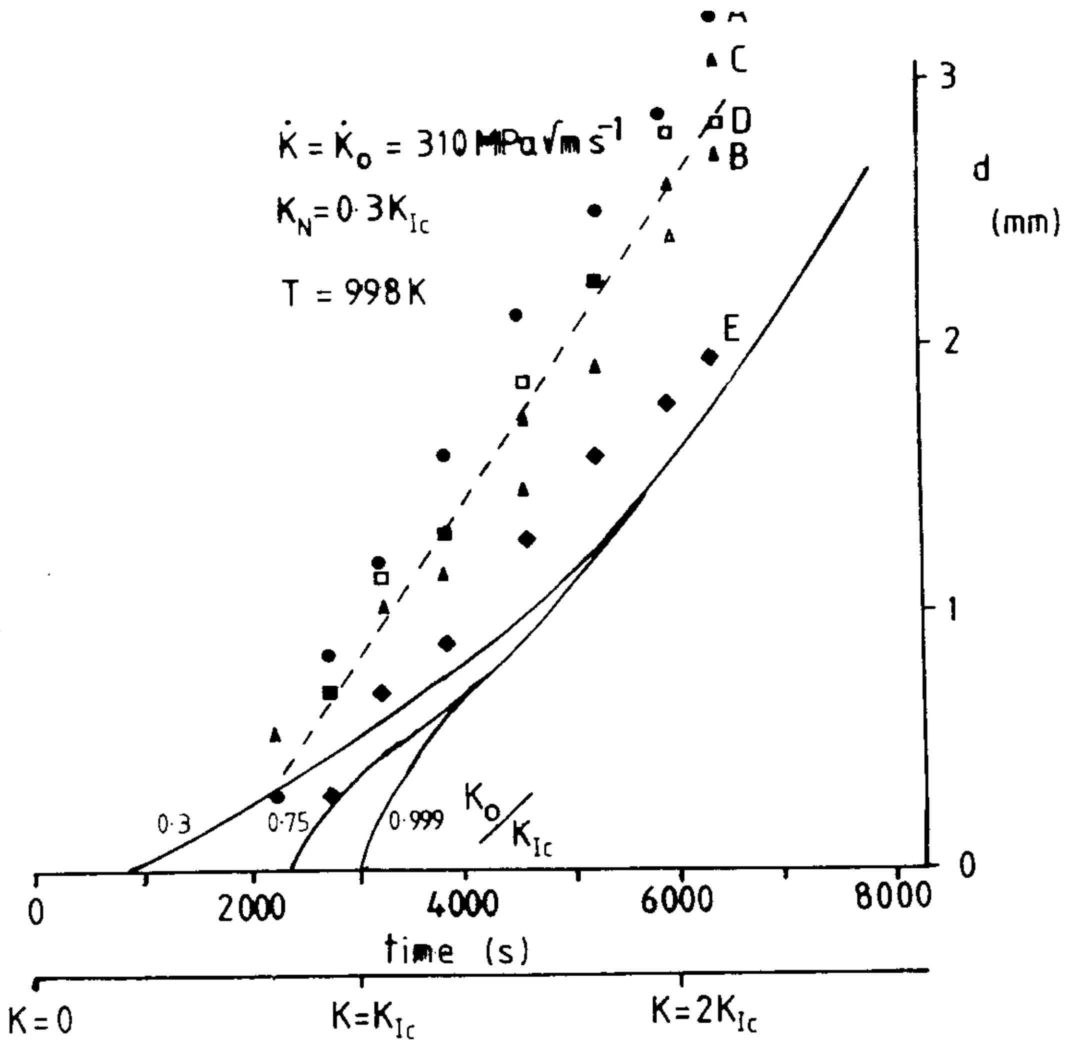

K̇ = K̇o = 310 MPa√m s⁻¹
KN = 0·3 KIc
T = 998 K
A
C
D
B
E
d (mm)
0·3
0·75
0·999
Ko/KIc
time (s)
K = 0
K = KIc
K = 2KIc


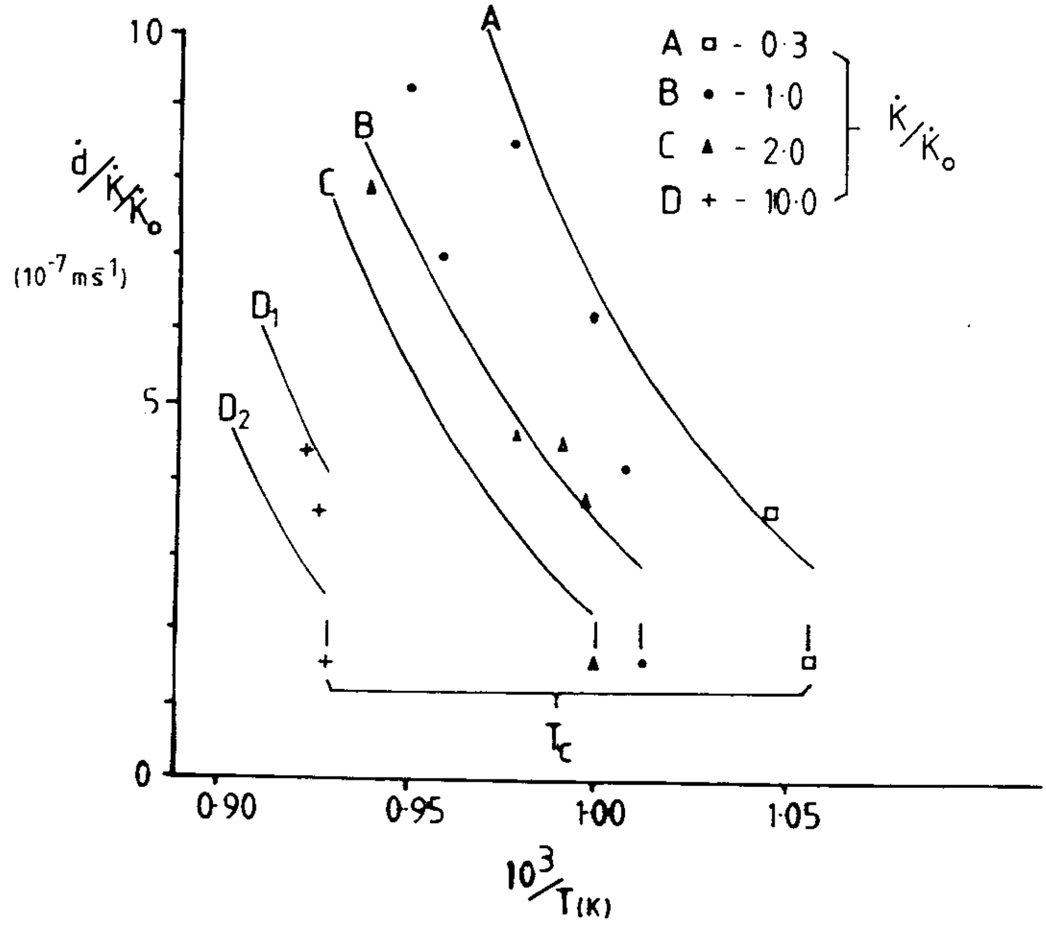

A - 0·3
B - 1·0
C - 2·0
D - 10·0
K̇/K̇o
ḋ/K̇/K̇o
(10⁻⁷ m s⁻¹)
A
B
C
D1
D2
Tc
10³/T(K)

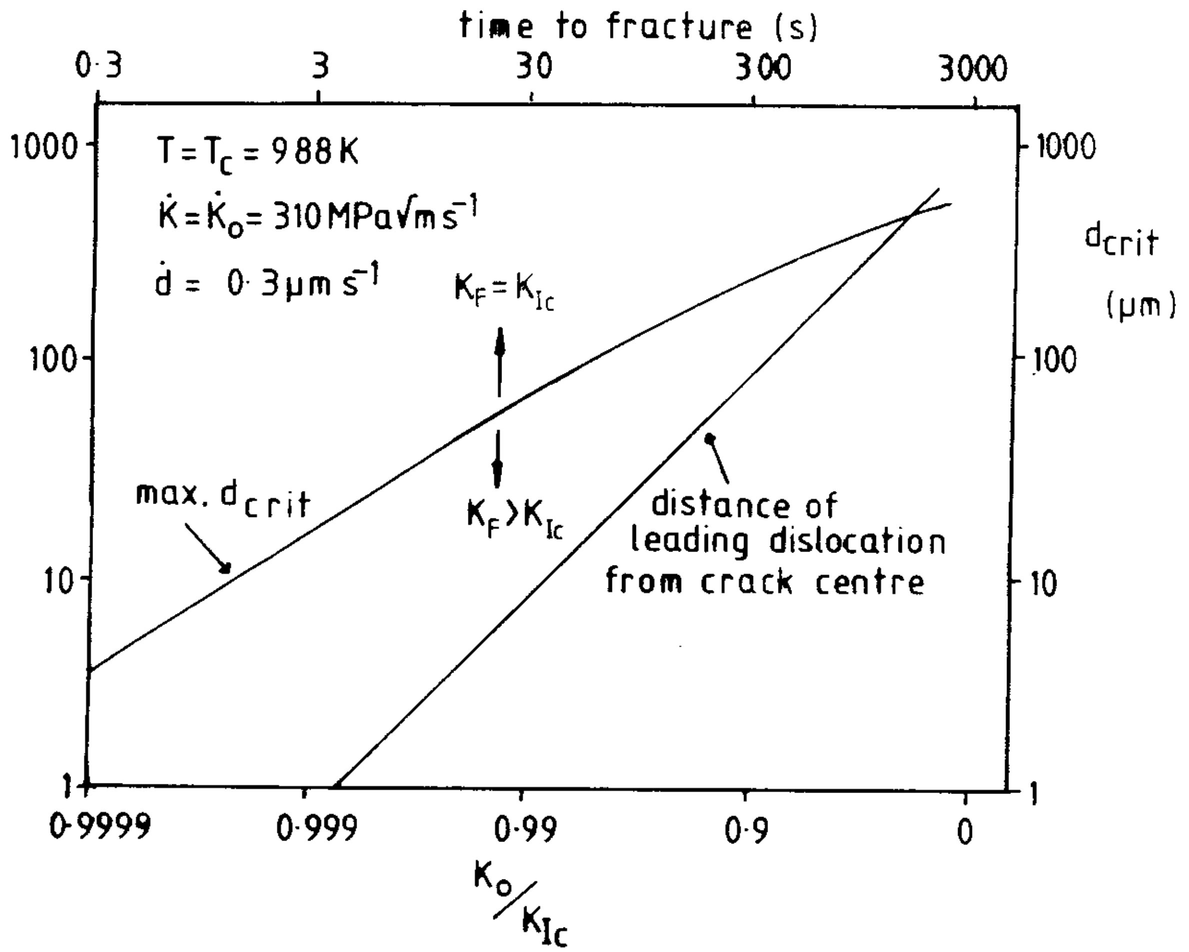
time to fracture (s)
0·3
3
30
300
3000
1000
100
10
1
$d_{crit}$
(μm)
$T = T_c = 988\,K$
$\dot{K} = \dot{K}_o = 310\,MPa\sqrt{m}\,s^{-1}$
$\dot{d} = 0{\cdot}3\,\mu m\,s^{-1}$
$K_F = K_{Ic}$
$K_F > K_{Ic}$
max. $d_{crit}$
distance of leading dislocation from crack centre
0·9999
0·999
0·99
0·9
0
$K_o / K_{Ic}$

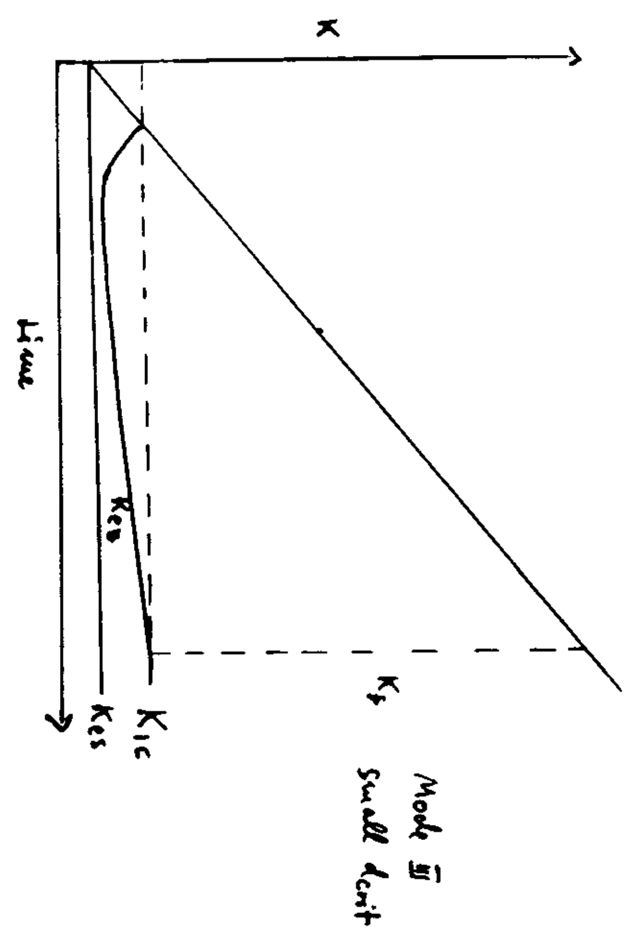
K
time
$K_{es}$
$K_{Ic}$
$K_f$
Mode III
small $d_{crit}$

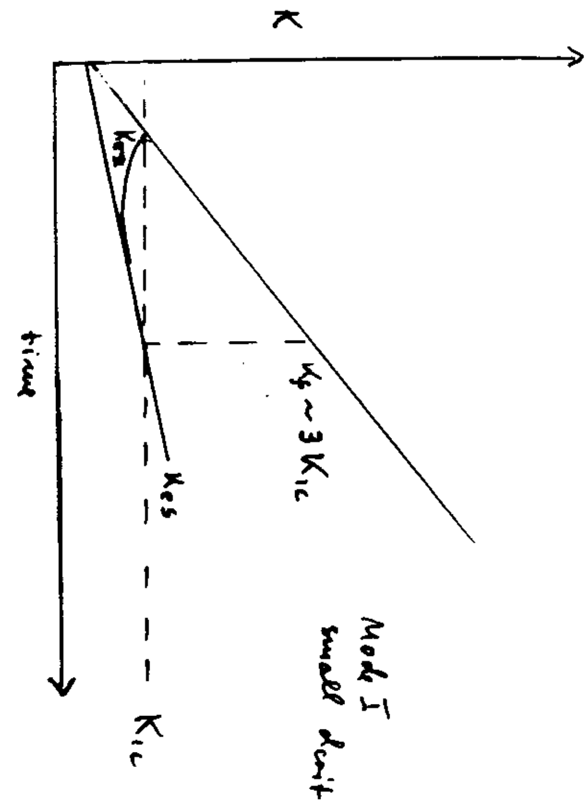
K
time
$K_{es}$
$K_{Ic}$
$K_f \sim 3\,K_{Ic}$
Mode I
small $d_{crit}$

## Warm Prestressing

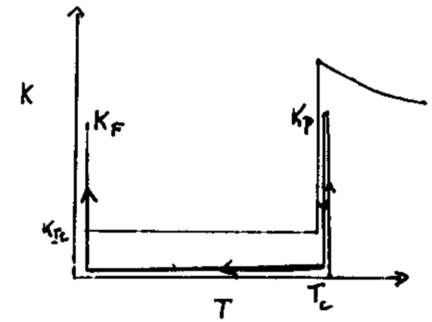


Stress Cycle

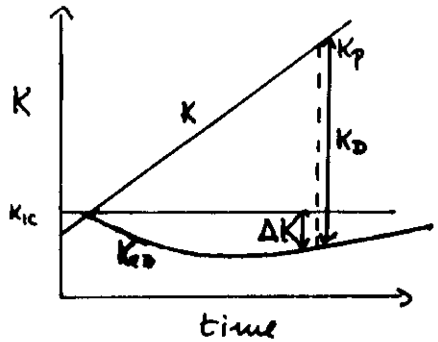


Model Calculation

If dislocation arrangement frozen in when unloading and cooling from high temperature

$$K_F = K_p + \Delta K = K_{Ic} + K_D$$

If relaxation occurs during cooling, $\Delta K$ could decrease and become negative, as $K_D$ decreases. $K_F$ will depend on loading/unloading cycle and cooling rate.

## Types of Transition

(no stable crack extension)

| | A | B | C | D |
|---|---|---|---|---|
| Original crack tip source spacing $2\,{}_id_{crit}$ | small ${}_id_{crit}\sim dfz$ | large | large | wide range |
| Existing dislocation density | (large) no effect | $K_d<K_{Ic}$ | $K_d>K_{Ic}$ no effect | $K_d>K_{Ic}$ no effect |
| Source nucleations along crack front for $K<K_{Ic}$; final spacing $2\,{}_fd_{crit}$ | ${}_fd_{crit}\sim{}_id_{crit}$ | small | small | ${}_fd_{crit}\sim{}_id_{crit}$ |
| Fracture criterion | $K_{ex}=K_{Ic}$ | $K_{ex}=K_{Ic}$ | $K_{ex}=K_{Ic}$ | $K_{ex}=K_{Ic}$ |
| Type of transition | gradual | sharp ${}_fd_{crit}$ controls | sharp ${}_fd_{crit}$ controls | gradual ${}_fd_{crit}$ controls |
| Factors determining $T_c$ | critical loop radius $X_c$, $K_N$, $\dot{K}/v_o$ | $K_d$, $r_o$, $\dot{K}/v_o$ | $K_N$, ${}_id_{crit}$, $\dot{K}/v_o$ | $K_N$, ${}_id_{crit}$, $\dot{K}/v_o$ |
| Possible examples | ? (not Si!) | Si Oxford | Si Göttingen? Nancy? | Si Oxford predeformed |

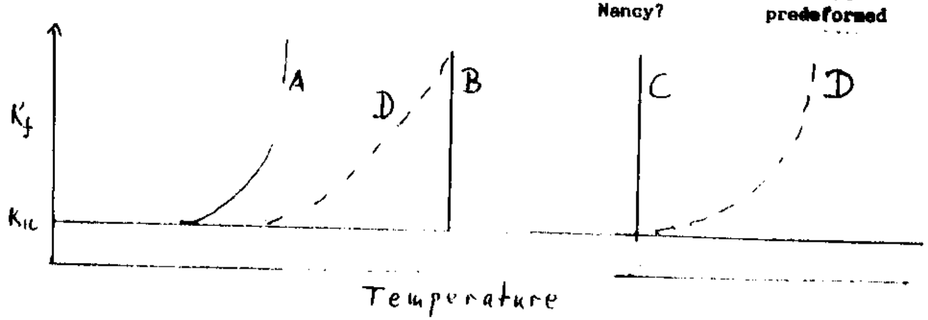

## Conclusions

1. Sharp transition due to nucleation of crack-tip sources at $K_o \sim K_{1c}$, which operate at $K_N << K_o$.

2. For sharp transitions, $T_c$ in a constant strain-rate test is determined by the time taken for the 'nucleation' event to occur. Two mechanisms have been proposed:

   (a) Nucleation of crack tip sources by existing dislocations moving to the crack tip and forming sources. $T_c$ is controlled by time taken for external dislocations to reach crack before $K \sim K_{1c}$; factors are $K_J (< K_{1c})$, $r_o$, $\dot{K}/v_o$; i.e. dependent on existing dislocation arrangement. Sharpness is controlled by $_r d_{crit}$.

   (b) Nucleation resulting from loops emitted from few special sites (spacing 2 $_l d_{crit}$) sweeping along crack front (Lüders type mechanism). $T_c$ is controlled by time taken for initial loops having moved $_l d_{crit}$ when $K = K_{1c}$; factors are $K_N$, $_l d_{crit}$, $\dot{K}/v_o$. Sharpness controlled by $_r d_{crit}$, $K_o$.

3. When crack tip sources are already present, and no nucleation occurs, transition is gradual. Likely to be the case when dislocation density is large (BCC metals?)

4. Strain-rate dependence of $T_c$ is controlled by activation energy controlling dislocation velocity, <u>not</u> activation energy for loop nucleation.